

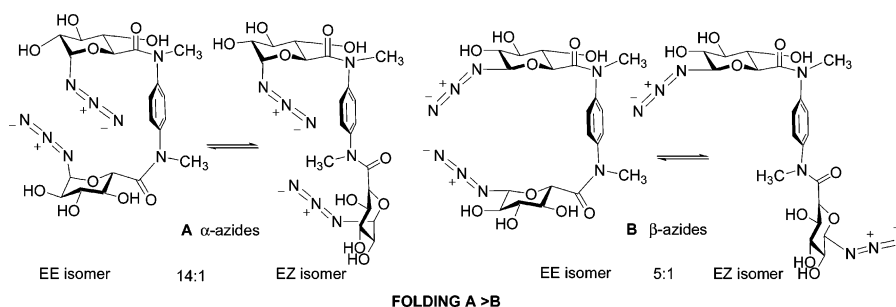
Synthesis of Structurally Defined Scaffolds for Bivalent Ligand Display Based on Glucuronic Acid Anilides. The Degree of Tertiary Amide Isomerism and Folding Depends on the Configuration of a Glycosyl Azide

Manuela Tosin and Paul V. Murphy*

Centre for Synthesis and Chemical Biology, Department of Chemistry, Conway Institute of Biomolecular and Biomedical Research, University College Dublin, Belfield, Dublin 4, Ireland

Paul.V.Murphy@ucd.ie

Received January 31, 2005



Syntheses and structural analyses of bivalent carbohydrates based on anilides of glucuronic acid are described. Secondary anilides predominantly adopted the *Z*-anti structure; there is also evidence for population of the *Z*-syn isomer. Bivalent tertiary anilides displayed two signal sets in their NMR spectra, consistent with the presence of (i) a major isomer where both amides have *E* configurations (*EE*) and (ii) a minor isomer where one amide is *E* and the other *Z* (*EZ*). Qualitative NOE/ROE spectroscopic studies in solution support the proposal that the anti conformation is preferred for *E* amides. The crystal structure of one bivalent tertiary anilide showed *E*-anti and *E*-syn structural isomers; intramolecular carbohydrate-carbohydrate stacking was observed and mediated by carbonyl-pyranose, azide-azide, and pyranose-aromatic interactions. The *EE* to *EZ* isomer ratio, or the degree of folding, for tertiary amides, was greatest for a bivalent compound containing two α -glycosyl azide groups; this was enhanced in water, suggesting that hydrophobic interactions are partially but not wholly responsible. Computational methods predicted azide-aromatic ($N\cdots H-C$ interaction) and azide-azide interactions for folded isomers. The close contact of the azide and aromatic protons ($N\cdots H-C$ interaction) was observed upon examination of the close packing in the crystal structure of a related monomer. It is proposed that the α -azide group is more optimally aligned, compared to the β -azide, to facilitate interaction and minimize the surface area of the hydrophobic groups exposed to water, and this leads to the increased folding. The alkylation of bivalent secondary anilides induces a switch from *Z* to *E* amide that alters the scaffold orientation. The synthesis of a bivalent mannoside, based on a secondary anilide scaffold, for investigation of mannose-binding receptor cross-linking and lattice formation is described.

1. Introduction

The use of pyranose scaffolds as peptidomimetics was first explored by Hirschmann, Nicolaou, Smith, and co-workers¹ and extended into other areas of bioorganic chemistry by these and other researchers.²⁻⁴ This research involves the placement or grafting of pharmacophoric groups onto the saccharide scaffold; the scaffold orients the attached groups in the direction of their

binding subsites. Herein, we describe an extension of this work that involves the placement of multiple recognition groups on pyranose-derived multivalent scaffolds generating novel multivalent ligands.^{5,6} Multivalent carbohydrates are of interest as they form part of a high-density coding system involved in a variety of biological processes^{6b} and are relevant for the development of new therapeutics⁷ or synthetic vaccines.⁸ There has been little pub-

lished work concerning the detailed 3D structures of bivalent or higher-order multivalent carbohydrate ligands. Recent indications show that multivalent carbohydrate ligands with increased rigidity⁹ or defined architecture¹⁰ can have enhanced affinity and selectivities. These observations suggest that detailed 3D structure–activity relationships will be interesting. The mechanisms of

action of multivalent ligands are complex¹¹ and include cross-linking of glycan-binding proteins that can result in the formation of soluble lattices that can alter receptor function at the cell surface.^{6e,12} For glycoclusters, it may be difficult to define bioactive conformations, assuming these exist, if flexible scaffolding is used for the display of the recognition components. The presentations of ligands preorganized on structurally defined scaffolds will be of interest. We have previously described the synthesis and structural analysis of bivalent *N*-glycosylbenzamides (**1,2**) in this context.¹³ The synthesis and structural analysis of secondary and tertiary anilides derived from glucuronic acid (**3,4**) is reported in the previous article.¹⁴ Herein, these studies are extended to the synthesis and structural analysis of **5**. The synthesis of a structurally

(1) (a) Hirschmann, R.; Nicolaou, K. C.; Pietranico, S.; Salvino, J.; Leahy, E. M.; Sprengeler, P. A.; Furst, G.; Smith, A. B., III; Strader, C. D.; Cascieri, M. A.; Candelore, M. R.; Donaldson, C.; Vale, W.; Maechler, L. *J. Am. Chem. Soc.* **1992**, *114*, 9217. (b) Nicolaou, K. C.; Salvino, J. M.; Raynor, K.; Pietranico, S.; Reisine, T.; Freidinger, R. M.; Hirschmann, R. In *Peptides—Chemistry, Structure, and Biology: Proceedings of the 11th American Peptide Symposium*; Rivier, J. E., Marshall, G. R., Eds.; ESCOM: Leiden, The Netherlands, 1990; pp 881–884. (c) Hirschmann, R.; Nicolaou, K. C.; Pietranico, S.; Leahy, E. M.; Salvino, J.; Arison, B. H.; Cichy, M. A.; Spoor, P. G.; Shakespeare, W. C.; Sprengeler, P. A.; Hamley, P.; Smith, A. B., III; Reisine, T.; Raynor, K.; Maechler, L.; Donaldson, C.; Vale, W.; Freidinger, R. M.; Cascieri, M. A.; Strader, C. D. *J. Am. Chem. Soc.* **1993**, *115*, 12550.

(2) (a) Wunberg, T.; Kallus, C.; Opatz, T.; Henke, S.; Schmidt, W.; Kunz, H. *Angew. Chem., Int. Ed.* **1998**, *37*, 2503. (b) Kallus, C.; Opatz, T.; Wunberg, T.; Schmidt, W.; Henke, S.; Kunz, H. *Tetrahedron Lett.* **1999**, *40*, 7783. (c) Opatz, T.; Kallus, C.; Wunberg, T.; Schmidt, W.; Henke, S.; Kunz, H. *Eur. J. Org. Chem.* **2003**, 1527. (d) Opatz, T.; Kallus, C.; Wunberg, T.; Kunz, H. *Tetrahedron* **2004**, *60*, 8613. (e) Hunger, U.; Ohnsmann, J.; Kunz, H. *Angew. Chem., Int. Ed.* **2004**, *43*, 1104. (f) Sofia, M. J. *Mol. Diversity* **1998**, *3*, 75. (g) Sofia, M. J.; Hunter, R.; Chan, T. Y.; Vaughan, A.; Dulina, R.; Wang, H. M.; Gange, D. *J. Org. Chem.* **1998**, *63*, 2802. (h) Sofia, M. J. *Med. Chem. Res.* **1998**, *8*, 362. (i) Sofia, M. J.; Silva, D. J. *Curr. Opin. Drug Discovery Dev.* **1999**, *2*, 365–376. (j) Silva, D. J.; Sofia, M. J. *Tetrahedron Lett.* **2000**, *41*, 855. (k) Jain, R.; Kamau, M.; Wang, C. G.; Ippolito, R.; Wang, H. M.; Dulina, R.; Anderson, J.; Gange, D.; Sofia, M. J. *Bioorg. Med. Chem. Lett.* **2003**, *13*, 2185. (l) Baizman, E. R.; Branstrom, A. A.; Longley, C. B.; Allanson, N.; Sofia, M. J.; Gange, D.; Goldman, R. C. *Microbiology (Reading, U.K.)* **2000**, *146*, 3129. (m) Ghosh, M.; Dulina, R. G.; Kakarla, R.; Sofia, M. J. *J. Org. Chem.* **2000**, *65*, 8387.

(3) (a) Hirschmann, R.; Hynes, J., Jr.; Cichy-Knight, M. A.; van Rijn, R. D.; Sprengeler, P. A.; Spoor, P. G.; Shakespeare, W. C.; Pietranico-Cole, S.; Barbosa, J.; Liu, J.; Yao, W.; Rohrer, S.; Smith, A. B., III. *J. Med. Chem.* **1998**, *41*, 1382. (b) Hirschmann, R.; Ducry, L.; Smith, A. B., III. *J. Org. Chem.* **2000**, *65*, 8307. (c) Wessel, H. P.; Banner, D.; Gubernator, K.; Hilpert, K.; Myller, K.; Tschopp, T. *Angew. Chem., Int. Ed. Engl.* **1997**, *36*, 751. (d) Moitessier, N.; Dufour, S.; Chrétien, F.; Thiery, J. P.; Maigret, B.; Chappleur, Y. *Bioorg. Med. Chem.* **2001**, *9*, 511. (e) Papageorgiou, C.; Haltiner, R.; Bruns, C.; Petcher, T. J. *Bioorg. Med. Chem. Lett.* **1992**, *2*, 135. (f) LeDiguarher, T.; Boudon, A.; Elwell, C.; Paterson, D. E.; Billington, D. C. *Bioorg. Med. Chem. Lett.* **1996**, *6*, 1983. (g) Cai, J. Q.; Davison, B. E.; Ganellin, C. R.; Thaisrivongs, S.; Wibley, K. S. *Carbohydr. Res.* **1997**, *300*, 109. (h) Dinh, T. Q.; Smith, C. D.; Du, X. H.; Armstrong, R. W. *J. Med. Chem.* **1998**, *41*, 981. (i) Moitessier, N.; Minoux, H.; Maigret, B.; Chrétien, F.; Chappleur, Y. *Lett. Pept. Sci.* **1998**, *5*, 75. (j) Zuccarello, G.; Bouzide, A.; Kvarnstrom, I.; Niklasson, G.; Svensson, S. C. T.; Brisander, M.; Danielsson, H.; Nilroth, U.; Karlen, A.; Hallberg, A.; Classon, B.; Samuelsson, B. *J. Org. Chem.* **1998**, *63*, 4898. (k) Hanessian, S.; Huynh, H. K. *Synlett* **1999**, *1*, 102. (l) Le Merrer, Y.; Poutout, L.; Depeay, J.-C. *Methods Mol. Med.* **1999**, *23*, 227. (m) Xuereb, H.; Maletic, M.; Gildersleeve, J.; Pelczar, I.; Kahne, D. *J. Am. Chem. Soc.* **2000**, *122*, 1883. (n) Kawato, H. C.; Nakayama, K.; Inagaki, H.; Ohta, T. *Org. Lett.* **2001**, *3*, 3451. (o) Liao, Y.; Li, Z. M.; Wong, H. N. C. *Chin. J. Chem.* **2001**, *19*, 1119. (p) Velasco-Torrijos, T.; Murphy, P. V. *Tetrahedron: Asymmetry* **2005**, *16*, 261. (q) Nakayama, K.; Kawato, H. C.; Inagaki, H.; Ohta, T. *Org. Lett.* **2001**, *3*, 3447. (r) The Versatile Assembly on Sugar Templates (VAST) program was initiated by the Alchemia Corp., see: Schliebs, D. *Mod. Drug Discovery* **2001**, *4*, 61. (s) Chery, F.; Cronin, L.; O'Brien, J. L.; Murphy, P. V. *Tetrahedron* **2004**, *60*, 6597. (t) Castoldi, S.; Cravini, M.; Micheli, F.; Piga, E.; Russo, G.; Seneci, P.; Lay, L. *Eur. J. Org. Chem.* **2004**, 2853. (u) Schweizer, F. *Trends Glycosci. Glycotechnol.* **2003**, *15*, 315. (v) Le, G. T.; Abbenante, G.; Becker, B.; Grathwohl, M.; Halliday, J.; Tometzki, G.; Zuegg, J.; Meuterms, W. *Drug Discovery Today* **2003**, *8*, 701. (w) Chery, F.; Murphy, P. V. *Tetrahedron Lett.* **2004**, *45*, 2067. (x) Nicolaou, K. C.; Trujillo, J. I.; Chibale, K. *Tetrahedron* **1997**, *53*, 8751.

(4) (a) Boer, J.; Gottschling, D.; Schuster, A.; Holzmann, B.; Kessler, H. *Angew. Chem., Int. Ed.* **2001**, *40*, 3870. (b) Von Roedern, E. G.; Kessler, H. *Angew. Chem., Int. Ed. Engl.* **1994**, *33*, 687. (c) Cipolla, L.; Forni, E.; Jimenez-Barbero, J.; Nicotra, F. *Chem.—Eur. J.* **2002**, *8*, 3976. (d) Peri, F.; Cipolla, L.; Forni, E.; Nicotra, F. *Monatsh. Chem.* **2002**, *133*, 369.

(5) Lee, Y. V.; Townsend, R. R.; Hardy, M. R.; Lönngrén, J.; Arnarp, J.; Haraldsson, M.; Lönn, H. *J. Biol. Chem.* **1983**, *258*, 199.

(6) For reviews on multivalency, see: (a) Mammen, M.; Choi, S.-K.; Whitesides, G. M. *Angew. Chem., Int. Ed.* **1998**, *37*, 2754. (b) Gabius, H.-J.; Siebert, H. C.; Andre, S.; Jimenez-Barbero, J.; Rudiger, H. *ChemBioChem* **2004**, *5*, 740. (c) Kiessling, L. L.; Gestwicki, J. E.; Strong, L. E. *Curr. Opin. Chem. Biol.* **2000**, *4*, 696. (d) Kiessling, L. L.; Strong, L. E.; Gestwicki, J. E. *Annu. Rev. Med. Chem.* **2000**, *35*, 321. (e) Brewer, C. F.; Miceli, M. C.; Baum, L. G. *Curr. Opin. Struct. Biol.* **2002**, *12*, 616. (f) Mulder, A.; Huskens, J.; Reinhoudt, D. N. *Org. Biomol. Chem.* **2004**, *3409*. (g) Pieters, R. J. *Trends Glycosci. Glycotechnol.* **2004**, *16*, 243. (h) Lindhorst, T. K. *Top. Curr. Chem.* **2002**, *218*, 201.

(7) Koeller, K. M.; Wong, C. H. *Nat. Biotechnol.* **2000**, *18*, 835.

(8) (a) Liebe, B.; Kunz, H. *Angew. Chem., Int. Ed. Engl.* **1997**, *36*, 618. (b) Hummel, G.; Schmidt, R. R. *Tetrahedron Lett.* **1997**, *38*, 1173. (c) Ragupathi, G.; Coltart, D. M.; Williams, L. J.; Koide, F.; Kagan, E.; Allen, J.; Harris, C.; Glunz, P. W.; Livingston, P. O.; Danishefsky, S. J. *Proc. Natl. Acad. Sci. U.S.A.* **2002**, *99*, 13699. (d) Verez-Bencomo, V.; Fernández-Santana, V.; Hardy, E.; Toledo, M. E.; Rodriguez, M. C.; Heynngnezz, L.; Rodriguez, A.; Baly, A.; Herrera, L.; Izquierdo, M.; Villar, A.; Valdés, Y.; Cosme, K.; Deler, M. L.; Montane, M.; Garcia, M.; Ramos, M.; Aguilar, A.; Medina, E.; Toran, G.; Sosa, L.; Hernandez, I.; Martínez, R.; Muzachio, R.; Carmenates, A.; Costa, L.; Cardoso, F.; Campa, C.; Diaz, M.; Roy, R. *Science* **2004**, *305*, 522.

(9) Vrasidas, I.; Andre, S.; Valentini, P.; Bock, C.; Lensch, M.; Kaltner, H.; Liskamp, R. M. J.; Gabius, H. J.; Pieters, R. J. *Org. Biomol. Chem.* **2003**, *1*, 803–810.

(10) (a) Gestwicki, J. E.; Cairo, C. W.; Strong, L. E. *J. Am. Chem. Soc.* **2002**, *124*, 14922. (b) Wittmann, V.; Seeberger, S. *Angew. Chem., Int. Ed.* **2000**, *39*, 4348. (c) Wittmann, V.; Seeberger, S. *Angew. Chem., Int. Ed.* **2004**, *43*, 900.

(11) (a) Gestwicki, J. E.; Cairo, C. W.; Strong, L. E.; Oetjen, K. A.; Kiessling, L. L. *J. Am. Chem. Soc.* **2002**, *124*, 14922. (b) Collins, B. E.; Paulson, J. C. *Curr. Opin. Chem. Biol.* **2004**, *8*, 617.

(12) (a) Andre, S.; Ortega, P. J. C.; Perez, M. A.; Roy, R.; Gabius, H.-J. *Glycobiology* **1999**, *9*, 1253. (b) Brewer, C. F. *Biochim. Biophys. Acta* **2002**, *1572*, 255.

(13) (a) Bradley, H.; Fitzpatrick, G.; Glass, W. K.; Kunz, H.; Murphy, P. V. *Org. Lett.* **2001**, *3*, 2629. (b) Murphy, P. V.; Bradley, H.; Tosin, M.; Pitt, N.; Fitzpatrick, G. M.; Glass, W. K. *J. Org. Chem.* **2003**, *68*, 5693.

(14) Tosin, M.; O'Brien, C.; Fitzpatrick, G. M.; Müller-Bunz, H.; Glass, W. K.; Murphy, P. V. *J. Org. Chem.* **2005**, *70*, xxx.

(15) One of the referees suggested that we explain why glycosyl azides were used. They were chosen for the ease and reliability with which they can be synthesized from readily available donors. Also, glycosyl azides are generally very stable under a wide range of reaction conditions, including acid and base. In addition, they are bioorthogonal and suitable for further functionalization should this be of interest in future.

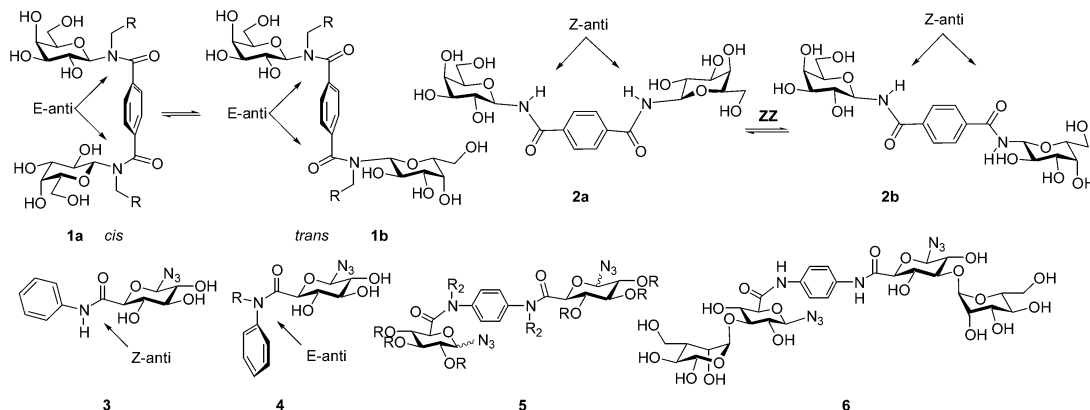
(16) Peto, C.; Batta, G.; Györgydeák, Z.; Sztaricskai, F. *Liebigs Ann. Chem.* **1991**, 505.

(17) Preliminary mechanistic studies have been reported: Murphy, P. V.; Poláková, M.; Pitt, N.; Tosin, M. Presented at the 22nd International Carbohydrate Symposium, Glasgow, U.K., July 2004, C44.

(18) The full experimental details are provided in the Supporting Information.

(19) Upreti, M.; Ruhela, D.; Vishwakarma, R. A. *Tetrahedron* **2000**, *56*, 6577.

(20) Kunz, H.; Waldmann, H. *Angew. Chem., Int. Ed. Engl.* **1984**, *23*, 71.

CHART 1. Structural Preferences Displayed by Bivalent Glycosylamides 1 and 2 and Glucuronic Acid Anilides 3 and 4, and the Structure of Scaffolding 5 and Bivalent Mannoside 6 Synthesized in This Study

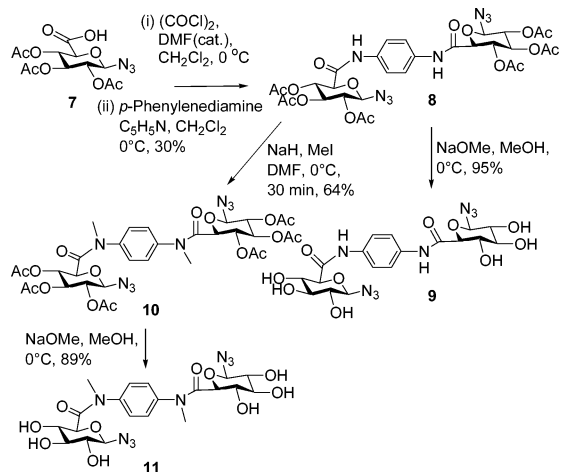
defined bivalent mannoside ligand **6**, with the potential to cross-link mannose-binding receptors, is described.

2. Results and Discussion

2.1. Synthetic Studies. 2.1.1. Synthesis of Novel Scaffolds.

The synthesis of **8–11** (Scheme 1) was carried out from acid **7**.¹⁴ This acid was first converted to the

SCHEME 1

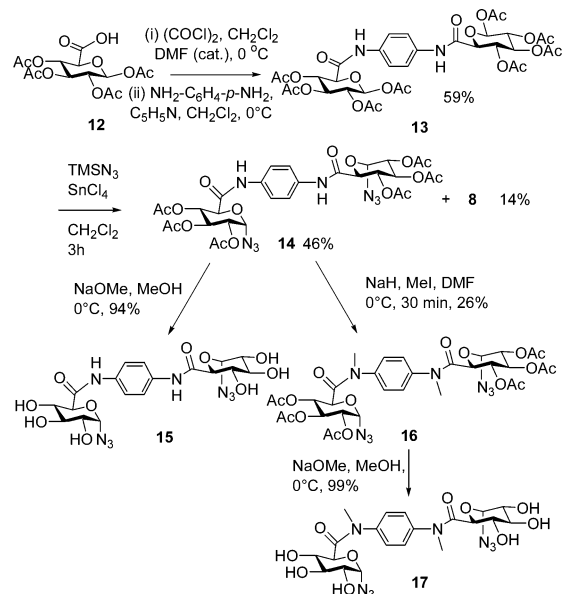


bivalent secondary amide **8** via reaction of its acid chloride with 1,4-phenylenediamine in the presence of pyridine in dichloromethane. Removal of the acetate protecting groups from **8** using catalytic sodium methoxide in methanol produced **9**, whereas methylation of **8** produced **10** and the subsequent deacetylation **11**.

The synthesis of **14** and **16–18**, in which the glycosyl azide groups¹⁵ have α -configurations, was carried out from **12** (Scheme 2). The bivalent amide **13** was first obtained via the coupling reaction of the acid chloride prepared from **12** and 1,4-phenylenediamine. The reaction of **13** with azidotrimethylsilane and SnCl₄¹⁶ in dichloromethane produced, after chromatography, a fraction containing a 77:23 mixture of **14**, a compound in which both anomeric azide groups have the α -configuration, and **8**. The stereoselectivity observed in this reaction was unexpected: the 1,2-*cis*-glycoside was preferentially obtained in the presence of the 2-acyl participating group. The mechanism involves anomerization of the initially formed β -azide.¹⁷ The deprotection of **14**

produced **15**, whereas alkylation of **14** using sodium hydride and iodomethane in DMF produced **16**, which was converted to **17** by deacetylation.

SCHEME 2

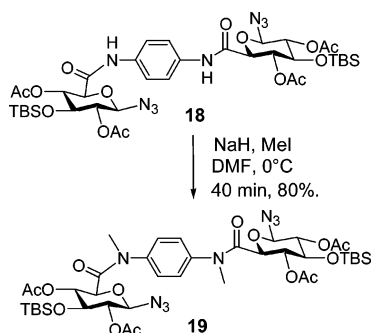


2.1.2. Synthesis of a Bivalent Mannoside.

The bis-silylated compound **18** was first synthesized¹⁸ as a potential intermediate to be used for the preparation of **6**. It can be converted to the bis-alkylated derivative **19** by a reaction with sodium hydride and iodomethane in DMF (Scheme 3). However the removal of the silyl groups from either **18** or **19** to produce the required acceptors for glycosidation was unsuccessful and resulted in mixtures.

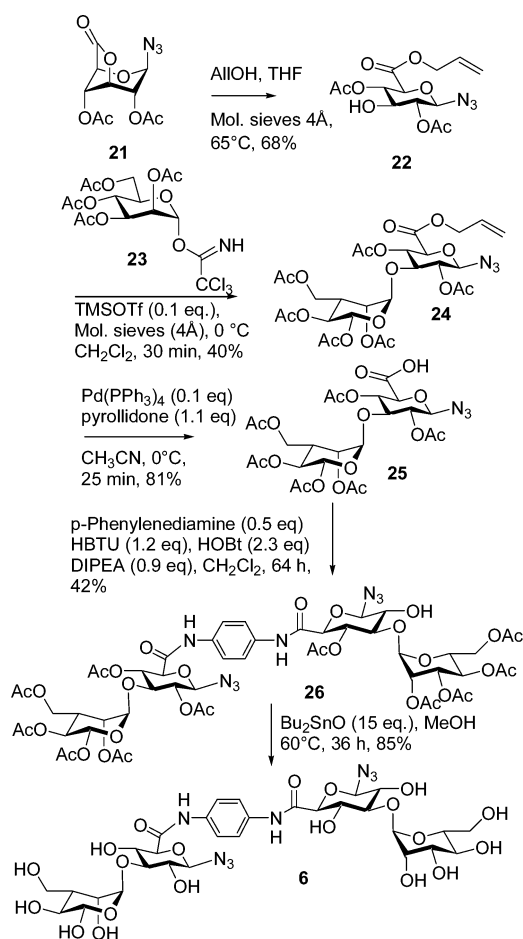
An alternative route was developed as shown in Scheme 4. The 6,3-lactone **21**¹⁴ reacts readily with allyl alcohol to produce **22**. The Schmidt glycosidation of **22** with **23**¹⁹ gave **24**. The allyl ester was removed by palladium catalysis to yield acid **25**.²⁰ The coupling of **26** with *p*-phenylenediamine promoted by HBTU/HOBt produced, after a prolonged reaction time, the protected divalent compound **26**. Removal of the acetate protecting groups by commonly used methods (NaOMe/MeOH, LiOH, and hydrazine) was unexpectedly problematic and resulted in a mixture containing unidentified products.

SCHEME 3



However, the use of dibutyltin oxide in methanol proved to be satisfactory for the removal of the acetates and gave **6**.²¹

SCHEME 4



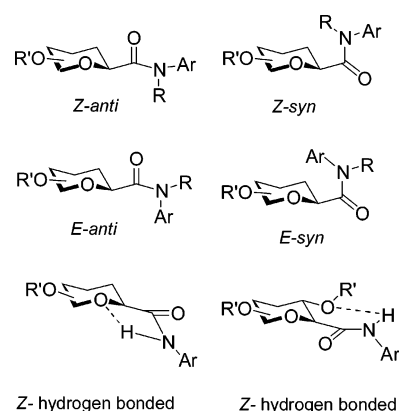
2.2. Structural Studies. A number of amide structural types (Chart 2)²² are relevant to the structure of

(21) The attempts to alkylate the amide of **26**, using sodium hydride and iodomethane as described for **8**, **14**, and **18**, were not successful in this case; they resulted in a complex mixture of products.

(22) The *E* and *Z* nomenclature refers to the amide configuration. For the *Z* isomer, the two groups of highest priority, according to Cahn Ingold Prelog rules (i.e., the aromatic group and oxygen atom), are on the same side of the bond with double bond character (amide bond); for the *E* isomer, these same two groups are on opposite sides of the amide bond. The syn and anti nomenclature refers to the torsion angle defined by H₅-C₅-C₆-O. For the anti isomer, this angle is 180 ± 90°; for the syn isomer, this angle is 0 ± 90°. *Z* hydrogen-bonded refers to the hydrogen-bonded structure observed in the crystal structure of **32**.

the scaffolds reported herein. The research described in the previous paper¹⁴ shows that secondary amides, such as **3**, prefer the *Z* configuration. The crystal structure (e.g., for **32**) and solid-state IR spectroscopic studies generally show that these amides can be involved in (intra- and intermolecular) hydrogen bonding in the solid state; IR spectroscopy indicates that this hydrogen bonding does not occur, in most cases, in solution. The ¹H NMR spectra of secondary amides recorded in solution show one signal set, assigned to the *Z* amide. This contrasted with tertiary anilide **4** which showed two signal sets. They were assigned to slowly interconverting *E*- and *Z*-amide isomers; the *E*-configured amide is more populated in solution (>85%). Qualitative NOE studies and molecular mechanics calculations supported the proposal that the *E*-anti structure is preferred for the monomers.

CHART 2. Amide Structure and Nomenclature



2.2.1. X-ray Crystal Structure of Dimer 10. The X-ray crystal structure of **10** was discussed in a recent communication.²³ One of the amides of **10** was found to be *E*-anti, whereas the other amide was *E*-syn. The structure can be considered folded as the carbohydrates stacked and adopted a cis or U-shaped conformation.²⁴ The stacking was mediated by noncovalent interactions. Interatomic distances that support intramolecular van der Waals interactions have been provided previously.²³ There were clear interactions (Figure 1) between (i) the oxygen atom of both pyranoses and the aromatic carbon and hydrogen atoms, (ii) the *E*-syn 2-acetate carbonyl oxygen atom and the *E*-anti pyranose ring protons, and (iii) the two azide groups.

2.2.2. NMR and IR Spectroscopic Analysis of Dimeric Compounds. One set of signals was observed for secondary amides (Table 1) by ¹H NMR (and ¹³C NMR) spectroscopy, consistent with the presence of only the *Z*-configured amide. The chemical shifts for the NH groups ($\delta_{\text{NH}} = 7.95\text{--}8.30$) of the protected compounds, recorded in CDCl₃, are consistent with those observed for monomeric compound **3** ($\delta_{\text{NH}} = 7.94\text{--}8.21$). The IR data (Table 2) for **8**, **13**, and **14** were also consistent with the data obtained for **3**; there is evidence for hydrogen bonding in the solid state (NH stretch <3350 cm⁻¹) but not in solution (NH stretch >3410 cm⁻¹). The ¹H NMR

(23) Tosin, M.; Müller-Bunz, H.; Murphy, P. V. *Chem. Commun.* **2004**, 494.

(24) The U-shaped conformation has the carbohydrate groups on the same side of the plane defined by the aromatic ring; the S-shaped conformation has the carbohydrates on opposite sides of the ring.

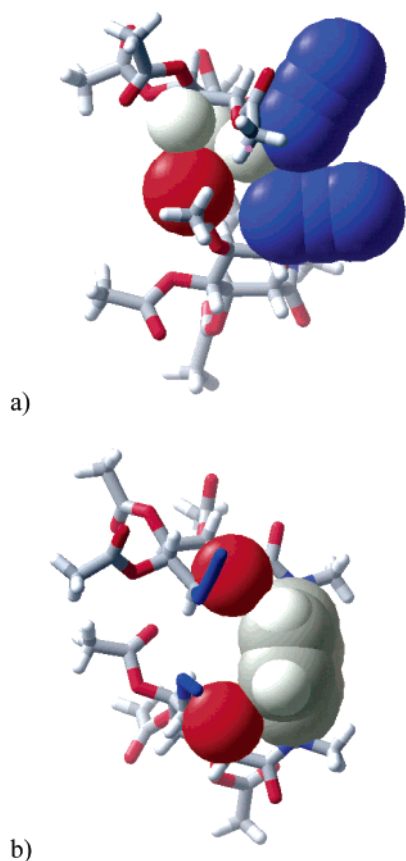


FIGURE 1. van der Waals surfaces were calculated using Macromodel 8.1 for the crystal structure of **10**. Shown are the (a) azide-azide and carbonyl-pyranose proton interactions and (b) pyranose oxygen-aromatic interactions.

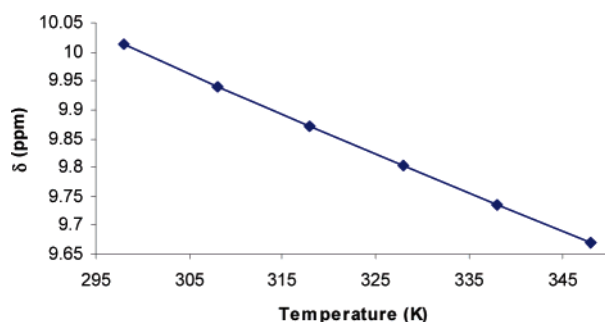


FIGURE 2. Temperature dependence of the NH shift of **9** in 10% D_2O/H_2O .

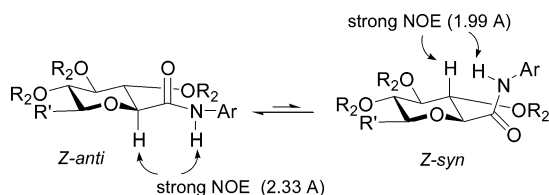


FIGURE 3. Summary of results from the NOE experiments for secondary amides **8**, **13**, **14**, and **18**.

spectrum recorded for **9** in D_2O/H_2O (10:90) showed a shift of the NH signal to a lower field ($\delta_{NH} = 10.01$) which suggests an increase in hydrogen bonding for the unprotected compounds. An upfield shift of this signal was observed with increasing temperature (Figure 2); the

estimated temperature coefficient, $\Delta\delta/\Delta T$, was -7.0 ppb/K and is significantly larger than that found for protected glucuronic acid anilides (-1.6 ppb/K) suggesting the engagement of the amide proton in an intermolecular hydrogen bond,²⁵ presumably with the solvent. The NOE spectroscopic studies of the secondary amides also showed results similar to those of **3**; strong NOE enhancements (Figure 3) of similar intensity were observed between the NH proton and both H-5 and H-4, and this suggests an equilibrium between the *Z*-anti and *Z*-syn isomers in solution. It is not possible to conclude that *Z*-syn is significantly populated on the basis of the NOE studies because the distance between NH and H-4 in this isomer would be 1.99 \AA and the distance between NH and H-5 in the *Z*-anti structure is 2.33 \AA .¹⁴ No NOE cross-peaks were observed between aromatic protons and H-2, H-4, or H-5 protons for secondary amides, ruling out the presence of *E*-anti and *E*-syn structures in solution. On the basis of the analogy with **3**, we propose that *Z*-anti is preferred in solution for all secondary amides and that *Z*-syn is populated to a lesser degree. The bivalent secondary anilide structure can be represented by **27a** and **27b** (Chart 3).

The observation of both *E*-syn and *E*-anti isomers in the crystal structure of tertiary amide **10** would indicate that two signal sets of equal intensity should be observed if this structure is stable in solution; however, this is not the case. There are multiple signal sets in the NMR spectrum of **10**, and these are assigned to two slowly interconverting configurational isomers. The first of these, the major isomer, is C_2 symmetric, whereas the second isomer is asymmetric. The NMR data for the C_2 symmetric isomer can be explained if (i) both amides of **10** adopt the *E*-anti structure (similar to U-shaped **30a** or S-shaped **30b**), (ii) both amides adopt the *E*-syn structure, or (iii) the *E*-anti to *E*-syn interconversion is dynamic but too rapid to be detected by NMR. Qualitative NOE data obtained for **10** in $CDCl_3$ indicate that *E*-anti amides are preferred: a strong NOE cross-peak is observed between H-5 of the sugar residue and the aromatic protons but not between the methyl group and H-4 or H-5. H-5 of the *E*-anti pyranose and H-4 of the *E*-syn pyranose were 3.16 and 2.51 \AA , respectively, from the nearest aromatic protons in the crystal structure of **10**; a significantly stronger NOE enhancement between H-4 and the aromatic protons than that between H-5 and the aromatic protons may, thus, have been expected if the *E*-syn isomer was populated, even to a minor extent. Irradiation of H-5 led to a strong positive enhancement of signals for H-1 and H-3 and to medium enhancements for H-4 and the aromatic protons. There were no enhancements of the H-5 or H-4 proton signal upon irradiation of the *N*-methyl signals as would have been expected if *Z*-anti or *Z*-syn were preferred isomers. The NMR data for the minor structural isomer are explained by an isomer with the general features of the unsymmetric L-shaped **30c**, i.e., there is one *E*-anti amide and one *Z*-configured amide. All other tertiary amides (**11**, **16**, **17**, and **19**) had NMR spectra (Table 1) similar to that of **10**.

(25) (a) Vasella, A.; Witzig, C. *Helv. Chim. Acta* **1995**, *78*, 1971. (b) Fowler, P.; Bernet, B.; Vasella, A. *Helv. Chim. Acta* **1996**, *79*, 269. (c) Stevens, E. S.; Sugawara, N.; Bonora, G. M.; Toniolo, C. *J. Am. Chem. Soc.* **1980**, *102*, 7048.

TABLE 1. Selected NMR Data^a for Anilides and Z/E Ratios for Tertiary Amides

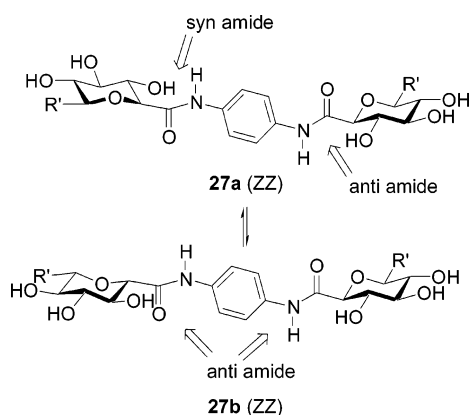
compd	δ (¹ H-NMR ^a)					NH	Z/E	EZ/EE
	H-1 ($J_{1,2}$) Z	H-1 ($J_{1,2}$) E	H-5 ($J_{4,5}$) Z	H-5 ($J_{4,5}$) E	H-5 ($J_{4,5}$) E			
6	4.98 (9.0)	—	4.24 (9.5)	—	nd		Z	—
8	4.87 (8.9)	—	4.15 (9.5)	—	8.30		Z	—
9	4.92 (8.8)	—	4.16 (9.5)	—	10.01 ^b		Z	—
10	4.73 (8.5)	4.22 (8.3)	4.56 (9.5)	4.11 (9.2)	—		1:4.6	1:1.8
11	4.89 (8.9)	4.53 (8.3)	nd	4.04 (9.7)	—		1:11	1:5
13	5.84 (7.5)	—	4.23 (9.4)	—	7.95		Z	—
14	5.76 (4.2)	—	4.47 (10.2)	—	8.09		Z	—
15	5.56 (4.1)	—	4.30 (9.6)	—	nd		Z	—
16	5.80 (br s)	5.63 (4.5)	4.95 (9.7)	4.45 (10.0)	—		1:9	1:4
17	5.68 (br s)	5.55 (4.4)	nd	4.27 (9.5)	—		1:29	1:14
18	4.65 (9.0)	—	4.00 (9.6)	—	7.99		Z	—
19	4.54 (8.9)	—	4.09 (8.9), 3.99(8.9)	4.32 (9.7)	4.02 (9.9), 3.88 (9.4)		—	1:6.7
26	4.73 (8.8)	—	4.04 (9.6)	—	8.01		Z	—
29	—	4.86 (3.3)	—	4.43 (9.3)	—		E	—
30	4.94 (br s), 5.04 (4.2)	4.97 (3.9)	4.17 (9.3), 5.08 (10.0)	4.40 (9.9)	—		1:12.3	—

^a NMR data recorded for protected compounds in CDCl₃ and for unprotected compounds in D₂O at 5 °C. ^b ¹H NMR spectrum recorded in 10:90 D₂O/H₂O.

TABLE 2. Infrared Spectroscopic Data

compd		IR (cm ⁻¹)		
		NH	-N ₃ asym.	C=O (amide)
8	solid state	3337.9	2124.5	1692.6
	CDCl ₃	3411.1	2122.5	1694.0
10	solid state	—	2121.5	1676.2
	CDCl ₃	—	2120.6	1674.2
11	solid state	—	2121.0	1667.9
13	solid state	3346.9	—	1682.3
	CDCl ₃	3410.8	2122.2	1695.4
14	solid state	—	2119.9	1702.5
	CDCl ₃	3418.4	2123.6	1673.4
16	solid state	—	2121.0	1672.3
	CDCl ₃	—	2121.0	1672.3
17	solid state	—	2121.9	1667.9
	CDCl ₃	—	2120.0	1673.4
19	solid state	—	2120.0	1673.4
	CDCl ₃	—	2120.6	1675.5

CHART 3



NOE enhancements similar to those described for **10** were observed for **11**, **16**, and **17** (Figure 4). However for **19**, the 2D-NOE spectra are more complex, and enhancements were observed which indicate that the *E*-syn isomer may have a higher population in this case. Evidence for dynamic interconversion of the *EE* and *EZ* structures was generally obtained by 1D- and 2D-NOESY/ROESY experiments,²⁶ as described for **3**¹⁴ and

(26) Both the NOESY and ROESY experiments had similar results for the cases where both techniques were investigated (e.g., **17**). The results were also consistent over a range of mixing times ($\tau_m = 0.4$ – 1.0 s).

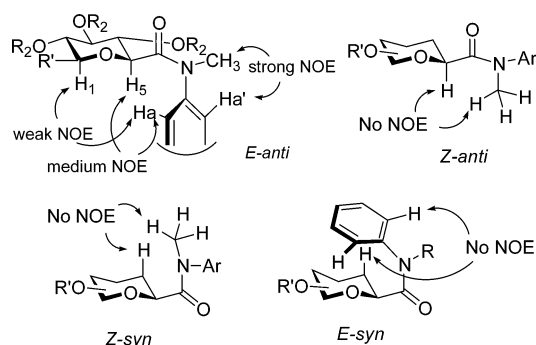


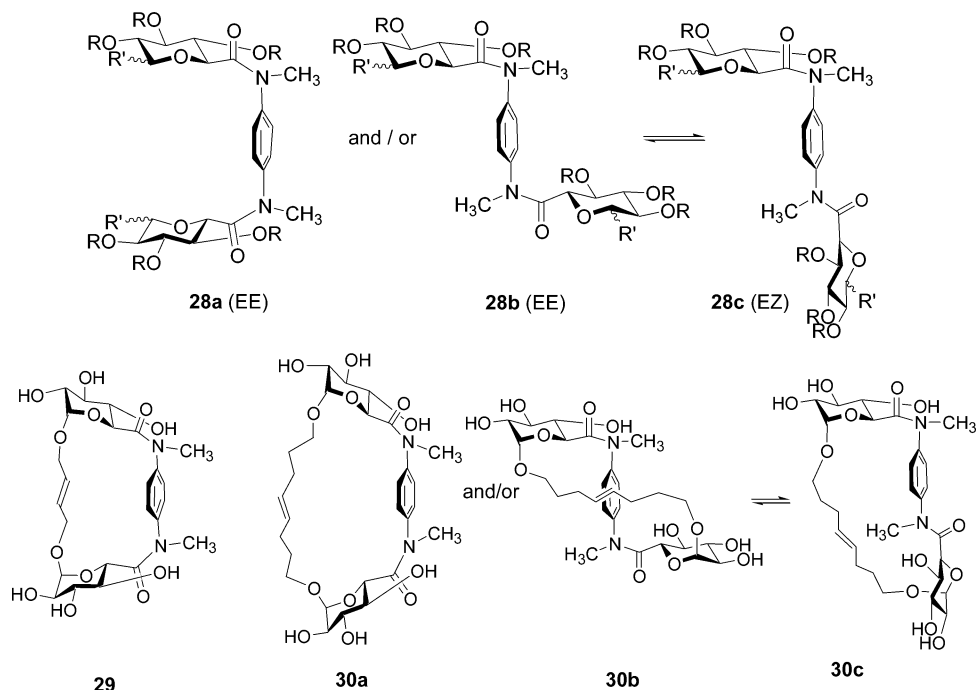
FIGURE 4. Summary of results from the NOE experiments for tertiary amides **10**, **15**, and **17**.

30,²⁸ and also by variable-temperature experiments. For example, the ¹H NMR spectrum of **17** displayed a signal at δ 3.51 (s), assigned to one *N*-methyl group of the *EZ* isomer, and a signal at δ 3.38 (s), assigned to the *N*-methyl group of the *EE* isomer; the 2D-NOESY and 2D-ROESY spectra showed a cross-peak with the same sign as the diagonal peaks between these two signals, and coalescence of these signals was observed in the ¹H NMR spectra recorded at 70 °C in D₂O. These experiments confirm that there is an exchange process occurring between the *E* and *Z* isomers. Similar phenomena were observed for the other signals (Table 1) of the bivalent tertiary amides. The chemical shifts of protons (H-5 and H-1) of the *E* isomer, in closest proximity to the aromatic ring, appear at a higher field than those of the *Z* isomer, a pattern that is consistent with that displayed by **4**.^{14,27} A structural study of the constrained macrocycles **29** and **30** (Chart 4) has been carried out²⁸ in parallel with the work described herein, and they show similar NMR spectroscopic behavior. Macrocycle **29** is sufficiently constrained so that only the *E*-anti amides²⁹ can be accessed, and therefore only one signal set was

(27) The NOE experiments for tertiary amides were generally carried out at 5 °C as broadening of signals often occurred at room temperature.

(28) (a) Velasco-Torrijos, T.; Murphy, P. V. *Tetrahedron: Asymmetry* **2005**, *16*, 261. (b) The crystal structure of **30c** has been determined and shows the L-shaped structure with both *E*-anti and *Z*-anti amides. Murphy, P. V.; Müller-Bunz, H.; Velasco-Torrijos, T. *Carbohydr. Res.* **2005**, *340*, 1437.

CHART 4. Structures of Bivalent Amides 28–30



observed in its ^1H NMR spectrum. Macrocycle **30** is more flexible and can access structures in which (i) both amides can be *E*-anti (**30a** and/or **30b**) or (ii) one is *Z*-anti and the other *E*-anti (**30c**),^{28b} in this case the ^1H NMR spectrum contains two signal sets, and they are assigned to the C_2 symmetric *EE* structural isomer and the *EZ* isomer (Table 1). The phase-sensitive NOESY and ROESY spectra for **29** and **30** showed cross-peaks similar to those described herein, and VT experiments confirmed the *E* to *Z* amide exchange process for **30** also.²⁸ It can be concluded, in general, that the *E*-anti isomer is preferred for the bivalent glucuronides described herein.

Integration of the signal sets in the ^1H NMR spectra thus gives *E/Z* or *EE/EZ* isomer ratios (Table 1) for the dimeric tertiary amides. There are some trends worth noting. The *EE/EZ* ratio is the highest for **17** at 14:1 (in D_2O at 5 $^\circ\text{C}$), whereas for **11** it is 5:1. This provides evidence for enhanced isomerization to the *EE*-amide structure in **17**. A similar trend is observed when comparing **10** and **16** where *EE/EZ* ratios in CDCl_3 are 1.8:1 and 4:1, respectively.³⁰ These observations also show that the population of the *E* amide (or *EE* amide) is enhanced if the azide group is axial rather than equatorial and is further enhanced in water (compared to chloroform) when no protecting groups are present.

The azide stretching frequencies for divalent compounds (Table 2) are consistent with those observed for **3** and **4**. Although **10** shows an azide–azide interaction in the solid state, there was no major alteration to the asymmetric azide stretching frequency. In general, the carbonyl stretch for secondary amides appeared at a higher frequency than that for tertiary amides.

(29) The U-shaped conformer is also expected to be strongly preferred because it was calculated to be 70 kJ/mol lower in energy than the S-shaped conformer.

(30) A similar trend was noted for monomeric analogues. See ref 10.

2.2.3. Conformational Analysis Using Molecular Modeling. Molecular modeling (Macromodel 8.5)³¹ was used to generate 3D models of the structural isomers accessible to the multivalent scaffolds. The crystal structure of **10**, which contained both the *E*-syn and *E*-anti amides, was optimized by DFT at the BLYP level of theory with the 6-31+G** basis set in Jaguar 5.0;³² there was no change to the geometry which indicates that it is a local minimum structure. This structure was used as the starting point for a Monte Carlo conformational search using the SUMM method in Macromodel;³³ the amide torsions were constrained so that only conformational isomers with *E* amides would be obtained. All isomers that were generated within 10 kJ/mol of the minimum-energy isomer had only the *E*-anti structure. Both U-shaped and S-shaped conformations (similar to **30a** and **30b**) of similar energies were generated. Low-energy structures for **11** and **17** were also generated by a similar conformational search. Selected conformers of **17** that had *E*-anti amides were further optimized by DFT at the BLYP level of theory with the 6-31+G** basis set in Jaguar 5.0, and these are shown in Figure 5. Parallel azide–aromatic–azide stacking is a feature of the S-shaped conformation, shown in Figure 5a. The azide group nitrogen atoms of this conformer are 5.0–5.3 Å from the aromatic group; this distance is too remote to propose that stabilization by van der Waals interactions occurs. Azide–aromatic stacking also occurs for a low-energy U-shaped conformer (Figure 5c) in which the azide and aromatic groups are in closer proximity (3.7–4.5 Å), indicating that closer packing of these groups might be possible. The carbohydrate–carbohydrate stack-

(31) Mohamadi, F.; Richards, N. G. J.; Guida, W. C.; Liskamp, R.; Lipton, M.; Caufield, C.; Chang, G.; Hendrickson, T.; Still, W. C. *J. Comput. Chem.* **1990**, *11*, 440.

(32) *Jaguar 5.0*; Schrödinger, LLC: Portland, OR, 1991–2003.

(33) Minimization was carried out using the Merck Molecular Force Field which gave the most accurate geometries for the azide groups.

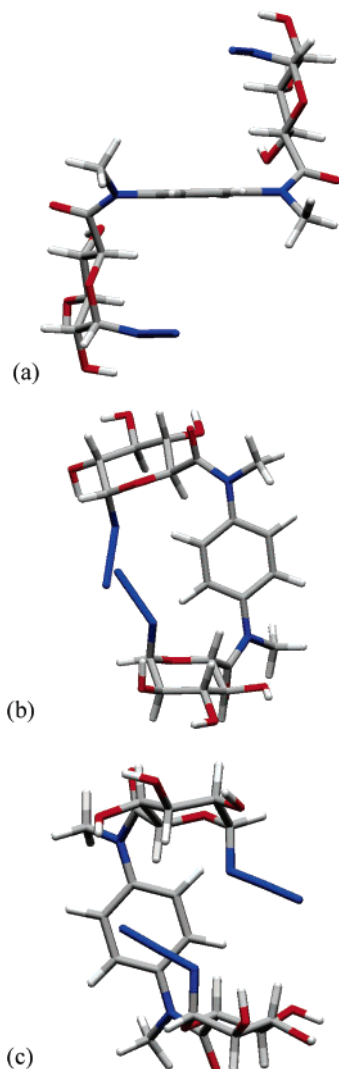


FIGURE 5. Low-energy conformers of **17**. (a) S-shaped conformer with azide–aromatic–azide stacking. (b) S-shaped conformer that has the terminal nitrogen atom of azide in contact with aromatic protons. Selected interatomic distances (Å): N–N = 3.25 and N–H = 3.01 and 3.43. (c) U-shaped conformer that shows azide–aromatic and azide–azide stacking.

ing observed is mediated by the azides since there are saccharide protons within 3.8 Å of the nitrogen atoms of the azide group. The alternative low-energy S-shaped conformer (shown in Figure 5b) shows that each terminal azide nitrogen atom is within 3.01 and 3.43 Å of the aromatic protons, suggestive of azide N \cdots H–C aromatic interactions, and within 3.25 Å of the other terminal azide nitrogen atom. Examination of the close packing in the crystal structure of **32**¹⁴ revealed that intermolecular N \cdots H–C aromatic interactions, similar to those calculated as described herein, are possible. The distances between the terminal azide nitrogen atom and the two closest aromatic hydrogen atoms were 2.84 and 3.07 Å in the X-ray structure (Figure 6).

There is a possibility of azide–carbohydrate and azide–aromatic interactions for **11**, but because of the directional properties of the azide, it would seem that a greater reorganization of the β -azide group than of the α -azide group would have to occur for these to be

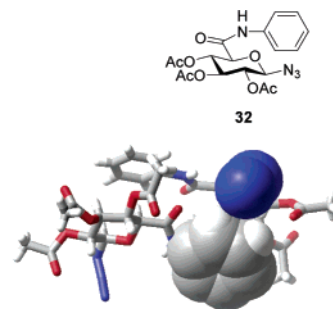


FIGURE 6. Structure of **32** and the van der Waals surfaces calculated using Macromodel for intermolecular azide–aromatic hydrogen interactions observed in the close-packed structure of **32**. Distances between the terminal azide nitrogen atom and the closest aromatic hydrogen atoms were 2.84 and 3.07 Å.

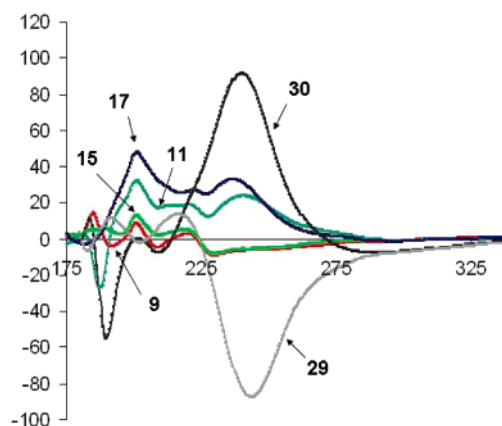


FIGURE 7. CD spectra for **9**, **11**, **15**, **17**, **29**, and **30**. See Table 3.

generated. Conformers with features, such as those in panels a–c of Figure 5, that minimize the surface area of water exposed to the hydrophobic surfaces more than other isomers may, thus, provide a basis for a hydrophobic effect which would enhance the folding of the divalent structures, and consequently, the *EE/EZ* ratio would be higher. The effect is not totally hydrophobic, as the NMR data would indicate, and some interaction of the azide groups with the aromatic ring, such as N \cdots H–C aromatic interactions, may be involved in enhancing the stabilization of the *EE* amide.

2.3. Circular Dichroism Studies. The circular dichroic (CD) spectra³⁴ of unprotected divalent compounds were recorded in water; these were compared with those of macrocycles **29** and **30**,²⁸ and the results are summarized in Table 3 and Figure 7. The pyranose groups of macrocycle **29** are constrained into a U-shape arrangement, and the spectrum of **29** shows positive maxima at 191.5 (¹B) and 214.5 nm (¹L_a) as well as a negative maximum of a significantly higher magnitude at 243.5 nm (¹L_b). In contrast, the spectrum of **30** has two negative maxima at 189.5 and 209.5 nm and a significant positive maximum at 240 nm for differential dichroic absorptions corresponding to same three $\pi \rightarrow p^*$ transitions. Macrocycle **30** is more flexible; it is potentially capable of

(34) McReynolds, K. D.; Gervay-Hague, J. *Tetrahedron: Asymmetry* **2000**, *11*, 337.

TABLE 3. UV and CD Spectroscopic Data

compd	conc (μM)	UV		CD	
		λ_{max} (nm), absorbance	λ (nm)	ellipticity (mdeg)	
9	49	198.0, 1.94 262.0, 1.02	184.5	+14.01	
			191.0	-4.00	
			200.5	+8.67	
			208.0	-4.63	
			220.0	+2.78	
11	46	194.0, 2.09 231.0, 0.79	245.5	-6.46	
			187.5	-27.02	
			194.5	+17.12	
			201.0	+32.30	
			214.0	+18.16	
15	49	202.0, 1.60 264.0, 1.08	220.5	+18.62	
			240.5	+23.63	
			183.5	+4.52	
			188.5	+5.65	
			201.0	+13.11	
17	93	198.9, 2.78 230.0, 1.25	218.0	+4.84	
			229.0	-8.18	
			241.0	-5.77	
			186.5	+4.56	
			202.5	+75.03	
29	25	240.0, 0.822	224.0	+50.95	
			236.0	+66.13	
			201.0	+47.86	
			221.5	+26.95	
			232.0	+32.70	
30	25	239.0, 1.08	236.5	+32.70	
			191.5	+32.1	
			214.5	+30.6	
			243.5	-87.0	
			189.5	-55.1	
			209.5	-7.8	
			240.0	+91.3	

adopting both U-shape and S-shape conformations where both amides are *E*-anti as well as a structure where one amide is *E*-anti and the other *Z*-anti. The CD spectrum of **30**, compared to that of **29**, could be interpreted as being a result of the S-shape arrangement being preferred. Both **11** and **30** have negative maxima at 187.5 and 189 nm, whereas **17** showed a small positive absorption at 186.5 nm. Apart from this difference, both **11** and **17** otherwise displayed similar profiles and showed positive maxima (at 240.5 and 241 nm) of lower intensity than **30**, indicating that they may have similar conformational preferences and that **11** and **17** preferentially adopt S-shaped structures. Significantly more experimental work would be required to confirm these proposals. The secondary amide derivatives **9** and **16** show CD spectra substantially different from those observed for the tertiary amides, in agreement with the proposal that the secondary and tertiary anilides have divergent secondary structures.

2.4. Summary and Conclusions. The synthesis and structure of novel multivalent scaffolds based on glucuronic acid anilides have been investigated. As for monomers, the structural preferences of the bivalent secondary anilides, which prefer *Z* amides, are different than those of the tertiary anilides, which prefer *E* amides. Alkylation of the amides leads, again, to configurational switching. Under such circumstances, the structural space or orientation of the carbohydrate residues of the secondary amides will diverge significantly from those of the tertiary amides. In addition to the configurational changes affected by the alkylation of amides, it should be possible to increase structural diversity further by using a dif-

ferent saccharide hydroxyl group to locate the binding groups.³⁵ The synthesis of **6** was carried out to illustrate an application of the scaffold to the synthesis of dimannosides for studies of their biological properties; the mannose groups are grafted to the 3-OH groups of the scaffold. Further synthesis and biological evaluation of bivalent ligands are underway, and the results of their biological evaluation will be reported in due course. The structural studies are relevant for the development of novel β -cyclodextrin³⁶ mimics; macrocycle **30** has shown the ability to bind to and reverse the quenching of fluorescence of a hydrophobic dye. The bivalent compounds based on glycosyl azides described herein do not display these phenomena. Macrocycle **29** has been proposed as a scaffold for development of α -helical peptidomimetics,³⁷ and azides **11** and **17** can access similar conformations. The anomeric substituent and its configuration alter the degree of isomerism of the amide and folding³⁸ of the divalent scaffold. Systems which are "molecular torsion balances"³⁹ are useful for the study of noncovalent interactions.⁴⁰ These studies are also relevant for the synthesis and structure of carbopeptoids and foldamers.⁴¹

3. Experimental Section

Preparation of 8. Oxalyl chloride (0.11 mL, 1.261 mmol) and DMF (0.15 mL) were added to **7** (408 mg, 1.182 mmol) in dichloromethane (18 mL) and at 0 °C under an atmosphere of N₂, and the mixture was stirred for 30 min while it was cooling on ice; the mixture was then stirred for a further 1 h at room temperature. *p*-Phenylenediamine (66 mg, 0.610 mmol) and pyridine (0.20 mL, 2.473 mmol) were stirred in dichloromethane (5 mL) in the presence of 4 Å molecular sieves until the amine had completely dissolved. The mixture containing the acid chloride was then cooled to 0 °C, and the solution containing the diamine was slowly added to it; the mixture was stirred for 30 min at 0 °C and for 2.5 h at room temperature. The mixture was washed with aq NaHCO₃ (20 mL); the organic layer was washed with 0.1 M HCl (20 mL), dried (Na₂SO₄), and filtered, and the solvent was removed to produce a yellow oil (250 mg). Chromatography (dichloromethane/EtOAc gradient elution) yielded **8** as a white solid (134 mg, 30%): $[\alpha]_{\text{D}} -51^\circ$ (*c* 0.5, CH₂Cl₂); ¹H NMR (300 MHz, CDCl₃) δ 8.30 (s, 2H, NH), 7.44 (s, 4H, aromatic H), 5.33 (t, 2H, *J*_{2,3} = 9.0, *J*_{3,4} = 9.0, H-3), 5.24 (t, 2H, H-4), 4.97 (t, 2H, *J*_{1,2} = 8.9, H-2), 4.87 (d, 2H, H-1), 4.15 (d, 2H, *J*_{4,5} = 9.5, H-5), 2.11, 2.08, 2.03 (each s, each 6H, each COCH₃); ¹³C NMR (500 MHz, CDCl₃) δ 169.8, 169.6, 169.2 (each s, each COCH₃), 163.7 (s, CONHAr), 133.4 (s, aromatic C), 121.4 (d, aromatic CH), 88.2 (d, C-1), 74.7, 71.8, 70.6, 69.1 (each d, C-2-C-5), 20.7, 20.6, 20.5 (each q, each COCH₃); FTIR (KBr) 3427, 2972, 2927, 2124, 175, 1691, 1517, 1375, 1237, 1069, 1039 cm⁻¹; FAB-HRMS found 785.1997, required 785.1990 [M + Na]⁺.

(35) Tosin, M.; Gouin, S. G.; Murphy, P. V. *Org. Lett.* **2005**, *7*, 211.

(36) Cyclodextrins have found wide application in pharmaceuticals: Davis, M. E.; Brewster, M. E. *Nat. Rev. Drug Discovery* **2004**, *3*, 1024.

(37) Velasco-Torrijos, T.; Murphy, P. V. *Org. Lett.* **2004**, *5*, 3961.

(38) Hill, D. J.; Mio, M. J.; Prince, R. B.; Hughes, T. S.; Moore, J. S. *Chem. Rev.* **2001**, *101*, 3893.

(39) (a) Paliwal, S.; Geib, S.; Wilcox, C. S. *J. Am. Chem. Soc.* **1994**, *116*, 4497. (b) Kim, E.-I.; Paliwal, S.; Wilcox, C. S. *J. Am. Chem. Soc.* **1998**, *120*, 11192.

(40) Hof, F.; Scofield, D. M.; Schweizer, W. B.; Diederich, F. *Angew. Chem., Int. Ed.* **2004**, *43*, 5056.

(41) (a) Nicolaou, K. C.; Florke, H.; Egan, M. G.; Barth, T.; Estevez, V. A. *Tetrahedron Lett.* **1995**, *36*, 1775. (b) Smith, M. D.; Long, D. D.; Claridge, T. D. W.; Fleet, G. W. J.; Marquess, D. G. *Chem. Commun.* **1998**, 2039. (c) Appella, D. H.; Christianson, L. A.; Klein, D. A.; Powell, D. R.; Huang, X.; Barchi, J. J., Jr.; Gellman, S. H. *Nature* **1997**, *387*, 381.

Preparation of 10. Sodium hydride (14 mg, 0.365 mmol, 60% dispersion in mineral oil) and methyl iodide (0.02 mL, 0.321 mmol) were added to an ice-cold solution of **8** (65 mg, 0.085 mmol) in DMF (2.7 mL) under an atmosphere of N₂, and the mixture was stirred for 30 min. Then, water and EtOAc were added, and the layers were separated; the organic layer was dried (Na₂SO₄), and the solvent was removed. Chromatography (dichloromethane/EtOAc gradient elution) yielded **10** as a white solid (43 mg, 64%): ¹H NMR (*EE* isomer, 300 MHz, CDCl₃) δ 7.42 (s, 4H, aromatic H), 5.50 (t, 2H, *J*_{3,4} = 9.4, H-4), 5.15 (t, 2H, *J*_{2,3} = 9.2, H-3), 5.24 (t, 2H, H-4), 4.87 (t, 2H, H-2), 4.22 (d, 2H, *J*_{1,2} = 8.3, H-1), 4.11 (d, 2H, *J*_{4,5} = 9.2, H-5), 3.35 (s, 6H, NCH₃), 2.02 (2s, 12H, overlapping COCH₃), 2.00 (s, 6H, COCH₃); ¹³C NMR (300 MHz, CDCl₃) δ 170.6, 169.3, 169.1 (each s, each COCH₃), 164.3 (s, CONMeAr), 142.6 (s, aromatic C), 129.0 (d, aromatic CH), 88.6 (d, C-1), 72.7, 72.4, 70.3, 69.7 (each d, C-2–C-5), 38.5 (q, NCH₃), 20.9, 20.8, 20.7 (each q, each COCH₃); selected ¹H NMR data (*EZ* isomer, 500 MHz, CDCl₃ at 0 °C) δ 4.73 (d, 1H, *J*_{1,2} = 8.5, H-1), 4.56 (d, 1H, *J*_{4,5} = 9.5, H-5), 3.57 (s, 6H, NCH₃); FTIR (KBr) 2936, 2120, 1756, 1670, 1511, 1435, 1369, 1237, 1074, 1039 cm⁻¹; FAB–HRMS found 813.2304, required 813.2303 [M + Na]⁺.

Preparation of 9. Deacetylation of **8** produced **9**: ¹H NMR (300 MHz, D₂O) δ 7.55 (s, 2H, Ar H), 4.92 (d, 1H, *J*_{1,2} = 8.8, H-1), 4.16 (d, 1H, *J*_{4,5} = 9.5, H-5), 3.73 (t, 1H, *J*_{3,4} = 9.3, H-4), 3.65 (t, 1H, *J*_{2,3} = 9.0, H-3), 3.40 (t, 1H, H-2); ¹³C NMR (500 MHz, D₂O) δ 171.3 (s, CONHAr), 136.4 (s, Ar C ipso), 125.9 (d, Ar CH), 93.1 (d, C-1), 80.0, 78.1, 75.2, 73.9 (each d, C-2–C-5); ES–HRMS found 533.1349, required 533.1357 [M + Na]⁺.

Preparation of 11. Deacetylation of **10** followed by purification via reverse-phase HPLC using a YMC-Pack C-4 (S 10 μm, 250 × 20 mm) reverse-phase column (isocratic elution H₂O/CH₃CN 70:30, flow rate 10 mL/min) produced **11**: ¹H NMR (*EE* isomer, 300 MHz, D₂O) δ 7.55 (s, 2H, Ar H), 4.53 (d, 1H, *J*_{1,2} = 8.3, H-1), 4.04 (d, 1H, *J*_{4,5} = 9.7, H-5), 3.81 (t, 1H, *J*_{3,4} = 9.3, H-4), 3.38 (s, 3H, NCH₃), 3.37 (t, 1H, H-2), overlapping with NMe), 3.28 (t, 1H, *J*_{2,3} = 9.0, H-3); ¹³C NMR (500 MHz, D₂O) δ 171.2 (s, CONHAr), 144.7 (s, aromatic C), 131.7 (d, aromatic CH), 93.2 (d, C-1), 77.7, 76.3, 75.1, 73.6 (each d, C-2–C-5), 40.7 (q, NCH₃); selected ¹H NMR data (*EZ*-isomer, 300 MHz, D₂O) δ 4.89 (d, 1H, *J*_{1,2} = 8.9, H-1), 3.57 (s, 3H, NCH₃); ES–HRMS found 561.1664, required 561.1670 [M + Na]⁺.

Preparation of 13. Acid **12** (474 mg, 1.31 mmol) was dissolved in dichloromethane (10 mL), and the mixture was cooled to 0 °C under N₂. Oxalyl chloride (0.11 mL, 1.31 mmol) and dry DMF (0.10 mL) were added, and the mixture was stirred for 30 min while it was cooling on ice; the mixture was then stirred for a further 1 h at room temperature and for a further 30 min at room temperature. *p*-Phenylenediamine (70 mg, 0.65 mmol) was stirred in dichloromethane (5 mL) in the presence of pyridine (0.22 mL, 2.72 mmol) and 4 Å molecular sieves until it had completely dissolved. The solution containing the diamine was added dropwise to the solution of the acid chloride at 0 °C, and the mixture continued to be stirred at this temperature for 30 min and for a further 2 h at room temperature. The reaction mixture was washed with saturated aq NaHCO₃ (15 mL) and dilute 0.1 M HCl (15 mL). The organic layer was dried (Na₂SO₄), and the solvent was removed. A solid residue was obtained which upon trituration in hot petroleum ether produced **13** (307 mg, 59%) as a white solid: [α]_D²⁵ (c 0.4, acetone); ¹H NMR (300 MHz, CDCl₃) δ 7.95 (s, 2H, NH), 7.43 (s, 4H, aromatic H), 5.84 (d, 2H, *J*_{1,2} = 7.5, H-1), 5.35 (m, 4H, H-3 and H-4, overlapping), 5.15 (m, 2H, *J*_{2,3} = 8.6, H-2), 4.23 (m, 2H, *J*_{4,5} = 9.4, H-5), 2.14, 2.09, 2.07, 2.03 (each s, each 6H, each COCH₃); ¹³C NMR (CDCl₃) δ 170.0, 169.8, 169.5, 169.1 (each s, each COCH₃), 164.3 (s, CONHAr), 133.7 (s, aromatic C), 121.3 (d, aromatic CH), 91.9 (d, C-1), 73.6, 72.1, 70.8, 68.9 (each d, C-2–C-5), 21.0, 20.9 (each q, each COCH₃), 20.8 (two q, each COCH₃, overlapping); FTIR (KBr) 3498, 2955,

2129, 1746, 1619, 1429, 1376, 1232, 1046, 901, 794, 601 cm⁻¹, FAB–HRMS found 819.2079, required 819.2072 [M + Na]⁺.

Preparation of 14. Azidotrimethylsilane (0.085 mL, 0.646 mmol) and tin(IV) tetrachloride (0.015 mL, 0.128 mmol) were added to a solution of **13** (100 mg, 0.126 mmol) in dry dichloromethane (5 mL), and the mixture was stirred for 3 h under an atmosphere of N₂. Aqueous NaHCO₃ (5 mL) was then added, and the biphasic mixture was stirred for 1 h. The layers were separated; the organic portion was dried (Na₂SO₄), and the solvent was removed. Chromatography of the residue (dichloromethane/EtOAc gradient elution) produced a white solid (58 mg, 60%), and NMR analysis showed that this was a 77:23 mixture of **14** and **8**: FAB–HRMS found 785.1989, required 785.1990 [M + Na]⁺. Analytical data for **14**: ¹H NMR (300 MHz, CDCl₃) δ 8.09 (s, 2H, NH), 7.46 (s, 4H, Ar H), 5.76 (d, 2H, *J*_{1,2} = 4.2, H-1), 5.48 (t, 2H, *J*_{2,3} = 9.8, *J*_{3,4} = 9.8, H-3), 5.18 (t, 2H, H-4), 4.94 (dd, 2H, H-2), 4.47 (d, 2H, *J*_{4,5} = 10.2, H-5), 2.12, 2.09, 2.04 (each s, each 6H, each COCH₃); ¹³C NMR (CDCl₃) δ 170.3, 170.0, 169.9 (each s, each COCH₃), 164.7 (s, CONHAr), 133.7 (s, aromatic C), 121.5 (d, aromatic CH), 86.3 (d, C-1), 70.3, 70.2, 69.4, 68.9 (each d, C-2–C-5), 20.9, 20.8, 20.7 (each q, each COCH₃); FTIR (KBr) 3410, 2962, 2124, 1756, 1696, 1660, 1519, 1370, 1224, 1047 cm⁻¹.

Preparation of 16. Sodium hydride (88 mg, 60% dispersion in mineral oil, 2.296 mmol) and methyl iodide (0.14 mL, 2.249 mmol) were added to an ice-cold solution of the 77:23 mixture of **14** and **8** (407 mg, 0.534 mmol) in DMF (17 mL) under an atmosphere of nitrogen. The reaction was judged to be complete after 30 min, and water and EtOAc were added; the layers were separated. The organic layer was dried (Na₂SO₄), and the solvent was removed; the residue was subjected to silica gel chromatography (dichloromethane/EtOAc gradient elution) to yield a 77:23 mixture of **16** and **10** (111 mg, 26%): FAB–HRMS found 813.2311, required 813.2303 [M + Na]⁺. Analytical data for **16**: ¹H NMR (300 MHz, CDCl₃) δ 7.43 (s, 4H, Ar H), 5.63 (d, 2H, *J*_{1,2} = 4.5, H-1), 5.52 (t, 2H, *J*_{3,4} = 9.7, H-4), 5.24 (t, 2H, *J*_{2,3} = 10.0, H-3), 4.90 (dd, 2H, H-2), 4.42 (d, 2H, *J*_{4,5} = 10.0, H-5), 3.37 (s, 6H, NCH₃), 2.04, 2.02, 1.98 (each s, each 6H, each COCH₃); ¹³C NMR (300 MHz, CDCl₃) δ 170.4, 170.1, 168.9 (each s, each COCH₃), 165.4 (s, CONMeAr), 142.8 (s, aromatic C), 129.5 (d, aromatic CH), 87.8 (d, C-1), 69.8, 69.7, 69.6, 67.2 (each d, C-2–C-5), 38.0 (q, NCH₃), 20.9, 20.8, 20.6 (each q, each COCH₃); FTIR (KBr) 2933, 2854, 2124, 1759, 1674, 1511, 1435, 1368, 1236, 1073, 1044 cm⁻¹.

Preparation of 15. The 77:23 mixture of **14** and **8** (0.069 g, 0.090 mmol) was deacetylated to produce **15** and **9** (0.043 g, 94%): ES–HRMS found 511.1550, required 511.1537 [M + H]⁺. Analytical data for **16**: ¹H NMR (300 MHz, D₂O) δ 7.42 (s, 4H, Ar H), 5.56 (d, 2H, *J*_{1,2} = 4.1, H-1), 4.30 (m, 2H, *J*_{4,5} = 9.6, H-5), 3.67 (dd, 2H, *J*_{2,3} = 9.8, H-2), 3.57 (m, 4H, H-3 and H-4 overlapping); ¹³C NMR (D₂O) δ 171.9 (s, CONHAr), 136.4 (s, Ar C), 125.8 (d, Ar CH), 92.2 (d, C-1), 76.2, 75.0, 74.0, 73.8 (each d, C-2–C-5).

Preparation of 17. The mixture containing **15** and **10** was deacetylated and purified by reverse-phase HPLC using a YMC-Pack C-4 reverse-phase (S 10 μm, 250 × 20 mm) column (isocratic elution H₂O/CH₃CN 80:20, flow rate 10 mL/min) to produce **17**: ES–HRMS found 561.1652, required 561.1670 [M + Na]⁺. Analytical data for the *EE* isomer: ¹H NMR (300 MHz, D₂O) δ 7.60 (s, 2H, aromatic H), 5.55 (d, 1H, *J*_{1,2} = 4.4, H-1), 4.27 (d, 1H, *J*_{4,5} = 9.7, H-5), 3.81 (t, 1H, *J*_{3,4} = 9.5, H-4), 3.69 (dd, 1H, *J*_{2,3} = 9.5, H-2), 3.45 (t, 1H, H-3), 3.38 (s, 3H, NCH₃); ¹³C NMR (500 MHz, D₂O) δ 171.8 (s, CONHAr), 145.1 (s, aromatic C), 131.9 (d, aromatic CH), 93.1 (d, C-1), 74.8, 73.5, 72.9, 72.2 (each d, C-2–C-5), 40.4 (q, NCH₃). Analytical data for the *EZ* isomer: selected ¹H NMR data (300 MHz, D₂O) δ 7.50 (s, 2H, Ar H), 5.68 (br s, 1H, H-1), 3.59 (s, 3H, NCH₃).

Preparation of Uronate 22. Lactone **21**¹⁴ (0.401 g, 1.406 mmol) was dissolved in freshly distilled THF (5 mL) in the presence of 4 Å molecular sieves, and allyl alcohol (0.19 mL, 2.794 mmol) was added. The solution was refluxed at 65 °C under N₂ overnight, then cooled to room temperature, and

filtered through Celite. Evaporation of the solvent under reduced pressure produced a crude brown-red material (0.6 g). Solid impurities were precipitated from dichloromethane and petroleum ether, and the evaporation of the mother liquor in vacuo produced **22** as a yellow oil (0.327 g, 68%): ^1H NMR (300 MHz, CDCl_3) δ 5.91 (m, 1H, $\text{CH}=\text{CH}_2$), 5.34 (m, 2H, $\text{CH}=\text{CH}_2$), 5.15 (t, 1H, $J_{3,4} = 9.3$, H-4), 4.87 (t, 1H, $J_{2,3} = 9.1$, H-2), 4.65 (m, 3H, $J_{1,2} = 8.8$, $\text{OCH}_2\text{CH}=\text{CH}_2$ and H-1), 4.07 (d, 1H, $J_{4,5} = 10.0$, H-5), 3.80 (t, 1H, H-3), 2.90 (b s, 1H, OH), 2.16, 2.09 (each s, each 3H, each COCH_3); ^{13}C NMR (CDCl_3) δ 170.5 (two s overlapping, each COCH_3), 166.4 (s, COOAll), 131.3 (d, $\text{CH}=\text{CH}_2$), 119.8 (t, $\text{CH}=\text{CH}_2$), 88.3 (d, C-1), 74.6, 73.3, 73.1, 71.7 (each d, C-2–C-5), 67.0 (t, $\text{OCH}_2\text{CH}=\text{CH}_2$), 21.0, 20.9 (each q, each COCH_3); FTIR (CH_2Cl_2 solution) 3431, 2957, 2120, 1753, 1432, 1375, 1230, 1082, 1039 cm^{-1} ; FAB–HRMS found 361.1361, required 361.1359 $[\text{M} + \text{NH}_4]^+$.

Preparation of 24. Trimethylsilyl triflate (1.5 mL of a 0.04 M solution in dry dichloromethane, 0.060 mmol) was added dropwise to an ice-cold solution of ester **22** (0.210 g, 0.612 mmol) and imidate **23** (0.301 g, 0.631 mmol) in freshly dried dichloromethane (15 mL) in the presence of 4 Å molecular sieves under a N_2 atmosphere. Within 30 min the reaction was complete; NaHCO_3 (~0.2 g) was added, and stirring was continued for 5 min. The mixture was then filtered and concentrated to produce a yellow foam (0.480 g); its purification by slow column chromatography (9:1 dichloromethane/EtOAc) produced disaccharide **24** as a white solid (0.165 g, 40%): R_f 0.47 (1:4 EtOAc/dichloromethane); mp 85–87 °C; $[\alpha]_{\text{D}}^{+12}$ (c 0.4, $(\text{CH}_3)_2\text{CO}$); ^1H NMR (300 MHz, CDCl_3) δ 5.92 (m, 1H, $\text{CH}=\text{CH}_2$), 5.32 (m, 4H, $\text{CH}=\text{CH}_2$, H-4' and H-4), 5.13 (m, 2H, $J_{2,3} = 3.4$, H-2' and H-3'), 5.01 (t, 1H, $J_{2,3} = 9.0$, H-2), 4.96 (d, 1H, $J_{1,2} = 1.8$, H-1'), 4.64 (m, 2H, $\text{OCH}_2\text{CH}=\text{CH}_2$), 4.56 (d, 1H, $J_{1,2} = 8.5$, H-1), 4.21 (dd, 1H, $J_{5,6a} = 4.0$, $J_{6a,6b} = 12.5$, H-6'a), 4.12 (m, 1H, H-6'b), 4.04 (d, 1H, $J_{4,5} = 9.8$, H-5), 3.97 (d, 1H, $J_{4,5} = 10.0$, $J_{5,6b} = 2.5$, H-5'), 3.90 (t, 1H, $J_{3,4} = 9.0$, H-3), 2.15, 2.14, 2.12, 2.12, 2.03, 1.96 (each s, each 3H, each COCH_3); ^{13}C NMR (CDCl_3) δ 170.8, 170.3, 169.9, 169.8, 169.7, 169.4 (each s, each COCH_3), 166.2 (s, COOAll), 131.3 (d, $\text{CH}=\text{CH}_2$), 119.9 (t, $\text{CH}=\text{CH}_2$), 99.7 (d, C-1'), 88.2 (d, C-1), 80.6, 74.6, 71.5, 70.0 (two signals overlapping), 69.6, 68.9, 65.4 (each d, C-2–C-5 and C-2'–C-5'), 67.0 (t, $\text{OCH}_2\text{CH}=\text{CH}_2$), 62.0 (t, C-6'), 21.1, 21.0, 20.9, 20.8 (signals overlapping), (each q, each COCH_3); FTIR (KBr) 2969, 2124, 1754, 1432, 1378, 1225, 1091, 1041 cm^{-1} ; FAB–HRMS found 696.1859, required 696.1854 $[\text{M} + \text{Na}]^+$.

(2,3,4,6-Tetra-O-acetyl- α -D-mannopyranosyl)-(1- \rightarrow 3)-2,4-di-O-acetyl- β -D-glucopyranuronosyl Azide 25. $\text{Pd}(\text{Ph}_3)_4$ (0.029 g, 0.025 mmol) and pyrrolidine (0.02 mL, 0.240 mmol) were added to an ice-cold solution of **24** (0.165 g, 0.245 mmol) in dry acetonitrile (1.5 mL). The reaction was judged complete within 25 min by TLC (1:4 EtOAc/dichloromethane); the mixture was filtered through Celite, and the solvent was removed to produce a yellow foam that was taken into EtOAc and washed with water. The two layers were separated, and the aqueous layer was acidified to pH 2 using Amberlite IR-120. The beads were filtered off, and the aqueous layer was extracted into EtOAc, then dried (Na_2SO_4), filtered, and evaporated in vacuo to produce **25** as a colorless syrup (0.125 g, 81%): ^1H NMR (300 MHz, CDCl_3) δ 5.33 (m, 2H, H-4' and H-4), 5.14 (m, 2H, H-3' and H-2'), 4.99 (m, 2H, H-1' and H-2), 4.74 (d, 1H, $J_{1,2} = 7.8$, H-1), 4.17 (m, 3H, H-6'a, H-6'b and H-5), 4.04 (m, 1H, H-5'), 3.96 (t, 1H, $J_{2,3} = 8.0$, $J_{3,4} = 8.0$, H-3), 2.49 (br s, 1H, OH), 2.22, 2.20, 2.18, 2.11, 2.11, 2.05 (each s, each 3H, each COCH_3); ^{13}C NMR (CDCl_3) δ 171.0, 170.3, 170.1, 169.9, 169.8, 169.3, 168.8 (each s, COCH_3 and COOH), 99.4 (d, C-1'), 87.7 (d, C-1), 80.0, 73.7, 71.3, 69.7, 69.7, 69.4, 68.8, 65.2 (each d, C-2–C-5 and C-2'–C-5'), 61.9 (t, C-6'), 21.0, 20.9,

20.7, 20.7, 20.6 (two signals overlapping) (each q, each COCH_3); FTIR (CH_2Cl_2 sol.) 3494, 3075, 2980, 2923, 2855, 2123, 1750, 1641, 1433, 1374, 1227, 1140, 1093, 1043 cm^{-1} ; FAB–HRMS found 678.1373, required 678.1371 $[\text{M} + 2\text{Na} - \text{H}]^+$.

Preparation of Diamide 26. Disaccharide **25** (0.081 g, 0.128 mmol), HOBt (0.040 g, 0.296 mmol), *p*-phenylenediamine (0.006 g, 0.055 mmol), and DIPEA (0.02 mL, 0.114 mmol) were dissolved in anhydrous dimethylformamide (0.8 mL) at 0 °C under a N_2 atmosphere. HBTU (0.060 g, 0.158 mmol) was added, and the reaction mixture was stirred for 1 h at 0 °C and then overnight at room temperature. The crude solution was then worked up with deionized water (10 mL) and EtOAc (10 mL): the organic layer was separated, dried (Na_2SO_4), filtered, and concentrated to produce a yellow oily residue. This was subjected to slow column chromatography (1:4 EtOAc/dichloromethane) to yield **26** as a white powder (0.030 g, 42%): R_f 0.61 (9:1 EtOAc/dichloromethane); ^1H NMR (300 MHz, CDCl_3) δ 8.01 (s, 2H, NH), 7.45 (s, 4H, Ar H), 5.32 (t, 2H, $J_{3',4'} = 10.0$, $J_{4',5'} = 10.0$, H-4'), 5.26 (t, 2H, $J_{3,4} = 9.0$, H-4), 5.14 (dd, 2H, $J_{2,3'} = 3.1$, H-3'), 5.08 (m, 2H, H-2'), 5.01 (apt s, 2H, H-1', overlapping with H-2), 5.01 (t, 2H, $J_{2,3} = 9.0$, H-2), 4.73 (d, 2H, $J_{1,2} = 8.8$, H-1), 4.22 (dd, 2H, $J_{5',6'a} = 3.8$, $J_{6'a,6'b} = 12.6$, H-6'a), 4.10 (m, 2H, H-6'b), 4.04 (d, 2H, $J_{4,5} = 9.6$, H-5), 3.97 (t, 2H, H-3), 3.97 (m, 2H, H-5', completely overlapped by H-3), 2.18, 2.16, 2.15, 2.12, 2.02, 1.95 (each s, each 6H, each COCH_3); ^{13}C NMR (CDCl_3) δ 170.8, 170.1, 170.0, 169.8, 169.7, 169.3 (each s, each COCH_3), 164.0 (s, CONH), 133.6 (s, Ar C), 121.9 (d, Ar CH), 99.4 (d, C-1'), 88.4 (d, C-1), 79.6, 75.2, 71.6, 70.4, 70.0, 69.7, 68.8, 65.7 (each d, C-2–C-5 and C-2'–C-5'), 62.2 (t, C-6'), 21.1, 21.0, 21.0, 20.9, 20.9, 20.8 (each q, each COCH_3); ES–HRMS found 1361.3748, required 1361.3681 $[\text{M} + \text{Na}]^+$.

Preparation of Diamide 6. Protected dimer **27** (7 mg, 5.23 μmol) and dibutyltin oxide (20 mg, 0.080 mmol) were suspended in dry methanol (1.5 mL) and refluxed at 60 °C for 36 h. The solvent was evaporated, and a white residue remained. This was partially redissolved in methanol (5 mL) and filtered. The filtrate was concentrated to a white powder (3.7 mg, 85%) which was further purified by reverse-phase HPLC using an YMC-Pack ODS-AQ reverse-phase (S 5 μm , 250 \times 20 mm) column and isocratic elution with H_2O and CH_3CN (85:15) (flow rate 10 mL/min): ^1H NMR (500 MHz, D_2O) δ 7.60 (s, 4H, Ar H), 5.35 (d, 2H, $J_{1,2'} = 1.4$, H-1'), 4.98 (d, 2H, $J_{1,2} = 9.0$, H-1), 4.24 (d, 2H, $J_{4,5} = 9.5$, H-5), 4.14 (m, 2H, H-2'), 4.06 (m, 2H, H-6'b), 3.96–3.86 (m, 10H, H-6'a, H-4', H-5', H-3', H-3), 3.81 (t, 2H, $J_{3,4} = 10.0$, H-4), 3.54 (t, 2H, $J_{2,3} = 9.0$, H-2); ^{13}C NMR (D_2O): δ 171.2 (s, CONH), 136.4 (s, Ar C), 125.9 (d, Ar CH), 103.8 (d, C-1'), 93.1 (d, C-1), 84.1, 79.9, 75.7, 74.4, 74.0, 73.2, 73.1, 69.3 (each d, C-2–C-5 and C-2'–C-5'), 63.5 (t, C-6'); ES–HRMS found 835.2626, required 835.2594 $[\text{M} + \text{H}]^+$.

Acknowledgment. The authors thank Geraldine Fitzpatrick (UCD) for NMR spectra, Dr. W. Kenneth Glass for assistance with IR spectra, Dr. Dilip Rai (UCD) for mass spectrometry measurements, and Joe Leonard and Thorri Gunnlaugsson at Trinity College Dublin for access to the CD spectrometer. Funding was provided by Enterprise Ireland (SC/00/182) and IRCSET (Ph.D. Scholarship to M.T.).

Supporting Information Available: NMR spectra, additional experimental procedures, molecular modeling coordinates, and crystallographic information file. This material is available free of charge via the Internet at <http://pubs.acs.org>.

JO050200Z